γ-ray emission from symmetric ordered nuclear spin structures at low temperatures

A. L. Allsop, G. J. Bowden,* N. Nambudripad, and N. J. Stone
Mullard Cryomagnetic Laboratory, Clarendon Laboratory,
University of Oxford, Oxford OX1 3PU, United Kingdom
(Received 14 August 1978)

The temperature dependence of γ-ray emission patterns from symmetric ordered nuclear-spin systems is discussed with particular reference to planar spin configurations. In particular, explicit expressions for "average statistical tensors" $\bar{\rho}_q^{\lambda}(I)$ are derived, for nuclear-spin structures with two-, three-, four-, and six-fold axes of symmetry. Several interesting identities are derived, which are useful aids in the analysis of a given nuclear orientation experiment. For example, if the nuclear structure possesses either a twofold or an effective twofold axis of symmetry, then the temperature isotherms for ρ_2^2 vs ρ_0^2 statistical-tensor diagrams are simply parallel straight lines.

I. INTRODUCTION

The problem of γ-ray emission from simple nuclear ferromagnets or antiferromagnets at low temperatures has recently been reviewed by Steffen and Alder.[1] In particular, these authors have shown that the angular distribution of γ rays may be characterized in terms of statistical tensors $\rho_q^{\lambda}(I_i)$, which describe the orientation of the nuclear ensemble. Explicit expressions for the special case of a nuclear assembly with axial symmetry have already been given, and the reader is referred to Steffen and Alder for more details.

In this paper we are concerned with the calculation of average statistical tensors $\bar{\rho}_q^{\lambda}(I)$ for symmetric nuclear-spin structures, other than simple ferromagnets or paramagnets. For simplicity, only spin structures which are essentially two dimensional in nature are considered, although the extension to more complicated spin structures are straightforward. Explicit expressions are derived for spin structures which possess either a two-, three-, four-, or six-fold axis of symmetry and the case of a helical spin structure is also examined. Special emphasis is placed on those assemblies which possess off-diagonal statistical tensors, $q \neq 0$.

II. BASIC EQUATIONS AND TRANSFORMATION TABLES

Following Steffen and Alder,[1] the angular distribution of γ rays from a point-source nuclear ensemble may be written

$$W(\theta,\phi)=\frac{d\Omega}{2\pi^{1/2}}\sum_{\substack{\lambda\\ \text{even}}}\sum_{q}(2I_i+1)^{1/2}\,(2\lambda+1)^{-1/2}A_{\lambda}(\gamma)\rho_q^{\lambda}(I_i)\,Y_{\lambda q}{}^{*}(\theta,\phi)\ , \tag{1}$$

where (i) I_i is the spin of the initial nuclear state; (ii) λ is the order of the multipole emission (for most practical purposes $\lambda=2$ and 4 only); (iii) $A_{\lambda}(\gamma)$ is a nuclear parameter which depends, in part, on the mixing ratio δ for $M1$ and $E2$; (iv) $\rho_q^{\lambda}(I_i)$ is a statistical tensor or state multipole (Fano[2,3]) which describes the orientation of the nuclear ensemble; and (v) $Y_{\lambda q}(\theta,\phi)$ is a spherical harmonic rank of λ.

The statistical tensors are calculated via the formula

$$\rho_q^{\lambda}(I_i)=\sum_m(-)^{I_i+m}\langle I_i-m\ I_i\ m'|\lambda q\rangle \times\langle I_i m|\,\underline{\rho}\,|I_i\ m'\rangle\ , \tag{2}$$

where $\langle I_i-m\ I_i\ m'|\lambda q\rangle$ is a Clebsch–Gordan coefficient and $\underline{\rho}$ is the density matrix for the nuclear ensemble in question. For example, if the nuclear ensemble is in thermal equilibrium we have

$$\underline{\rho}=e^{-\beta H}/\mathrm{Tr}(e^{-\beta H})\ . \tag{3}$$

On making use of the Hermitian nature of the density matrix $\underline{\rho}$, together with the symmetry properties of the Clebsch–Gordan coefficient, it can be shown that

$$\rho_q^{\lambda}(I_i)^{*}\equiv(-)^q\rho_{-q}^{\lambda}(I_i)\ . \tag{4}$$

Consequently, Eq. (1) may be rewritten

$$W(\theta,\phi)=\frac{\delta\Omega}{2(\pi)^{1/2}}\sum_{\lambda_{\text{even}}}(2I_i+1)^{1/2}(2\lambda+1)^{-1/2}A_\lambda(\gamma)\Big[\rho_0^\lambda(I_i)\,Y_{\lambda 0}(\theta,\phi)+\sum_{q>0}\{\rho_q^\lambda(I_i)[Y_{\lambda q}(\theta,\phi)]^*+(-)^q[\rho_{+q}^\lambda(I_i)]^*[Y_{\lambda -q}(\theta,\phi)]^*\}\Big], \tag{5}$$

which reveals that the angular distribution function may be characterized in terms of statistical tensors $\rho_q^\lambda(I_i)$ with $q\geq 0$.

In many instances, however, the Hamiltonian describing the nuclear ensemble is such that statistical tensors with odd q are identically equal to zero. This is the situation, for example, if the magnetic hyperfine field at the nucleus coincides with one of the axes of the electric-quadrupole interaction. For many purposes therefore we may write

$$\begin{aligned}W(\theta,\phi)=(\delta\Omega/4\pi)\{1&+A_2(\gamma)(2I_i+1)^{1/2}[\rho_0^2\,\tfrac{1}{2}(3\cos^2\theta-1)+\rho_2^2(\tfrac{3}{2})^{1/2}(1-\cos^2\theta)\cos 2\phi]\\&+A_4(\gamma)[\rho_0^4\,\tfrac{1}{8}(35\cos^4\theta-30\cos^2\theta+3)+\rho_2^4\,\tfrac{1}{2}(\tfrac{5}{2})^{1/2}(1-\cos^2\theta)(7\cos^2\theta-1)\cos 2\phi\\&+\rho_4^4\,\tfrac{1}{4}(\tfrac{35}{2})^{1/2}(1-\cos^2\theta)^2\cos 4\phi]\},\end{aligned} \tag{6}$$

where the series has been terminated at $\lambda=4$ and $\rho_q^\lambda(I_i)$ has been replaced by the abbreviation ρ_q^λ.

The usefulness of the statistical-tensor formulation of the γ-ray problem lies in their transformation properties under spatial rotations. Following a rotation of the coordinate system through the Euler angles α,β,γ, the new statistical tensors $\rho_q^{\lambda\prime}$, referred to the new primed axes, are related to those referred to the old axes, via the matrix equation

$$\rho_m^{\lambda\prime}=\sum_{m'}\mathfrak{D}_{m'm}^\lambda(\alpha,\beta,\gamma)\rho_{m'}^\lambda\ . \tag{7}$$

The $\mathfrak{D}_{m'm}^\lambda(\alpha,\beta,\gamma)$ are the well-known rotation matrices (e.g., Edmonds[4])

$$\mathfrak{D}_{m'm}^\lambda(\alpha,\beta,\gamma)=e^{im'\alpha}d_{m'm}^\lambda(\beta)e^{im\gamma} \tag{8}$$

and explicit expressions for $d_{m'm}^2(\beta)$ and $d_{m'm}^4(\beta)$ may be seen in Tables I and II respecively, together with a brief resumé of their symmetry properties.

TABLE I. Rotation matrices $d_{m'm}^2(\beta)$.

$$d_{2\pm 2}^2(\beta)=\tfrac{1}{4}(1\pm\cos\beta)^2$$
$$d_{2\pm 1}^2(\beta)=\tfrac{1}{2}\sin\beta(1\pm\cos\beta)$$
$$d_{20}^2(\beta)=\tfrac{1}{2}(\tfrac{3}{2})^{1/2}\sin^2\beta$$
$$d_{00}^2(\beta)=\tfrac{1}{2}(3\cos^2\beta-1)$$

Symmetry properties

$$d_{m'm}^\lambda(\beta)=(-)^{m'-m}d_{-m'-m}^\lambda(\beta)$$
$$d_{m'm}^\lambda(\beta)=(-)^{m'-m}d_{mm'}^\lambda(\beta)$$

III. TWOFOLD SYMMETRIC NUCLEAR-SPIN CONFIGURATIONS

As an introduction, consider the simple two-spin arrangement shown in Fig. 1(a). In this example two nuclear spins, confined to the x-y plane, make an angle of $\pm\beta$ with respect to the x axis. Moreover, since the angular distribution γ rays from nuclei with angles $\pi+\beta$ and β are identical, we may focus our attention on determining the γ-ray emission pattern for the twofold symmetric spin configuration of Fig. 1(b).

Next we assert that the Hamiltonian for each nucleus can be written in the simple form

$$H_n=A\vec{I}\cdot\hat{U}_n+P[I_z^2-\tfrac{1}{3}I(I+1)]\ , \tag{9}$$

where A and P are the magnetic and quadrupole hyperfine parameters, respectively, and $\hat{U}_n$ is a unit vector in the direction of the internal magnetic hyperfine field. In general, of course, the nuclear

TABLE II. Rotation matrices $d_{mm'}^4(\beta)$.

$$d_{4\pm 4}^4(\beta)=\tfrac{1}{16}(1\pm\cos\beta)^4$$
$$d_{4\pm 3}^4(\beta)=\frac{1}{4(2)^{1/2}}\sin\beta(1\pm\cos\beta)^3$$
$$d_{4\pm 2}^4(\beta)=\frac{(7)^{1/2}}{8}\sin^2\beta(1\pm\cos\beta)^2$$
$$d_{4\pm 1}^4(\beta)=\tfrac{1}{4}(\tfrac{7}{2})^{1/2}\sin^3\beta(1\pm\cos\beta)$$
$$d_{40}^4(\beta)=\tfrac{1}{8}(\tfrac{35}{2})^{1/2}\sin^4\beta$$
$$d_{2\pm 2}^4(\beta)=\tfrac{1}{4}(1\pm\cos\beta)^2(7\cos^2\beta\mp 7\cos\beta+1)$$
$$d_{2\pm 1}^4(\beta)=\frac{1}{4(2)^{1/2}}\sin\beta(1\pm\cos\beta)(14\cos^2\beta\mp 7\cos\beta-1)$$
$$d_{20}^4(\beta)=\tfrac{1}{4}(\tfrac{5}{2})^{1/2}(1-\cos^2\beta)(7\cos^2\beta-1)$$
$$d_{00}^4(\beta)=\tfrac{1}{8}(35\cos^4\beta-30\cos^2\beta+3).$$

Hamiltonian may be more complicated than that of Eq. (9). However, provided P is nonzero, H_n will give rise to off-diagonal statistical tensors ρ_q^λ, so Eq. (9) is a suitable introduction to the more general case.

To make further progress it is advantageous to adopt a new frame of reference, where the new z axis coincides with the direction of the magnetic field $\hat{U}_n$, as shown in Fig. 1(c). With respect to this co-ordinate system

$$H_n = AI_z + P\{-\tfrac{1}{2}[I_z^2 - \tfrac{1}{3}I(I+1)] + \tfrac{1}{2}(I_+^2 + I_-^2)\} \ , \tag{10}$$

where we have $z = (z'', z''')$ for nuclei a and b, respectively. Statistical tensors ρ_q^λ for this Hamiltonian have been tabulated in the previous paper by Bowden *et al.*,[5] for all values of A and P, and $1 \leq I \leq 8$. Consequently, the problem has been reduced to one of relating the individual sets of statistical tensors, associated with each nucleus (a,b), to a common frame of reference.

This is most easily achieved using the transformation properties of statistical tensors under spatial rotations of the co-ordinate system. Specifically, the rotation matrices required, for rotations of $\pm\beta$ about the x′ axis of Fig. 1(c), are obtained by setting the Euler angles $\alpha = \gamma = \frac{1}{2}\pi$ and $\beta = \pm\beta$ in Eq. (8), and Tables I and II, respectively. With respect to the (x',y',z') frame of reference we have

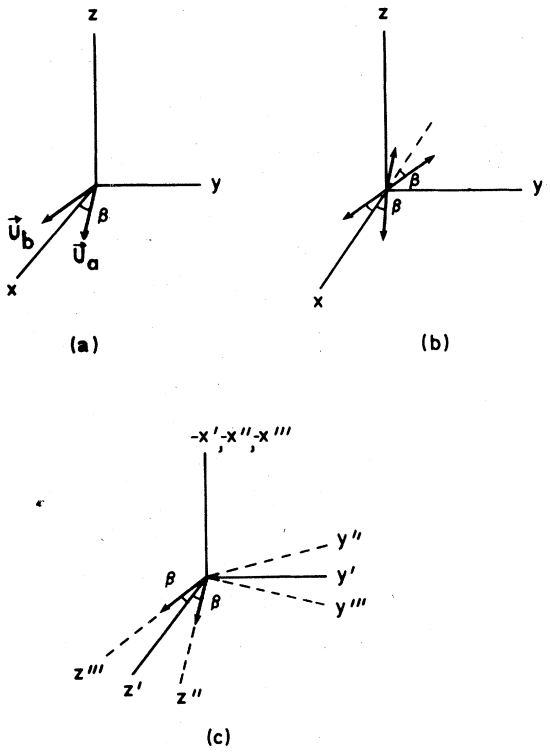

FIG. 1. Twofold symmetric nuclear-spin structure.

$$\begin{pmatrix} \rho_2^{2'} \\ \rho_1^{2'} \\ \rho_0^{2'} \\ \rho_{-1}^{2'} \\ \rho_{-2}^{2'} \end{pmatrix}_a = \begin{pmatrix} d^2_{22}(\beta) & -d^2_{21}(\beta) & d^2_{20}(\beta) & -d^2_{2-1}(\beta) & d^2_{2-2}(\beta) \\ -d^2_{12}(\beta) & d^2_{11}(\beta) & -d^2_{10}(\beta) & d^2_{1-1}(\beta) & -d^2_{1-2}(\beta) \\ d^2_{02}(\beta) & -d^2_{01}(\beta) & d^2_{00}(\beta) & -d^2_{0-1}(\beta) & d^2_{0-2}(\beta) \\ -d^2_{-12}(\beta) & d^2_{-11}(\beta) & -d^2_{-10}(\beta) & d^2_{-1-1}(\beta) & -d^2_{-1-2}(\beta) \\ d^2_{-22}(\beta) & -d^2_{-21}(\beta) & d^2_{-20}(\beta) & d^2_{-2-1}(\beta) & d^2_{-2-2}(\beta) \end{pmatrix} \begin{pmatrix} \rho_2^2 \\ 0 \\ \rho_0^2 \\ 0 \\ \rho_{-2}^2 \end{pmatrix} \ , \tag{11}$$

where use has been made of the identities

$$(\rho_2^2)_a = (\rho_{-2}^2)_a = \rho_2^2 \ , \tag{12}$$

$$(\rho_1^2)_a = (\rho_{-1}^2)_a = 0 \ , \tag{13}$$

and

$$(\rho_0^2)_a = \rho_0^2 \ , \tag{14}$$

for the Hamiltonian defined by Eq. (10).

A similar matrix equation can be derived for nuclear moment number 2, with β replaced by $-\beta$. Consequently, on defining an average statistical tensor

$$\bar{\rho}_q^{2'} = \tfrac{1}{2}[(\rho_q^2)_a' + (\rho_q^2)_b'] \ , \tag{15}$$

we find

$$\bar{\rho}_2^{2'} \equiv \bar{\rho}_{-2}^{2'} = \rho_2^2(1 - \tfrac{1}{2}\sin^2\beta) - \rho_0^2 \tfrac{1}{2}(\tfrac{3}{2})^{1/2}\sin^2\beta \ , \tag{16}$$

$$\bar{\rho}_1^{2'} = \bar{\rho}_{-1}^{2'} = 0 \ , \tag{17}$$

and

$$\bar{\rho}_0^{2'} = -\rho_2^2(\tfrac{3}{2})^{1/2}\sin^2\beta + \rho_0^2 \tfrac{1}{2}(3\cos^2\beta - 1) \tag{18}$$

per nucleus. These would be the actual values of $\bar{\rho}_2^2$ and $\bar{\rho}_0^2$ determined from a nuclear-orientation experiment, using the angular-distribution function $W(\theta,\phi)$ of Eq. (6).

As an example, we show in Fig. 2, a family of $\bar{\rho}_2^{2'}$ vs $\bar{\rho}_0^{2'}$ curves for various angles β between the two nuclear spins. In preparing this diagram, we have made use of the tabulated statistical tensors ρ_2^2 and ρ_0^2, for the special case of $I = 3$ and $x = 0.5$, where $[((\frac{1}{4})) \equiv 0$ for integer I and $\frac{1}{4}$ for half-integer I]

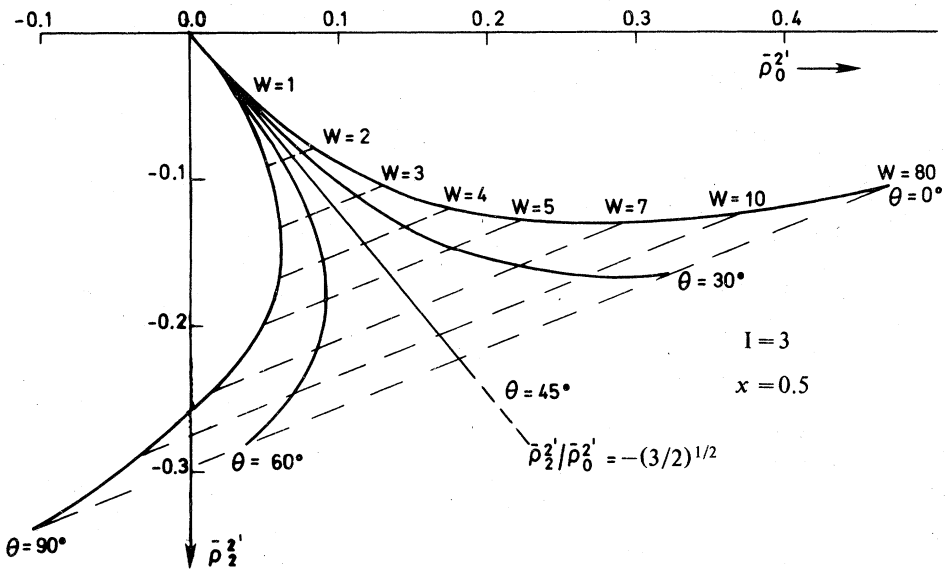

FIG. 2. Statistical tensor plot of $\bar{\rho}_2^{2'}$ vs $\rho_0^{2'}$ for a twofold symmetric nuclear-spin structure with $\beta=0°$, 30°, 45°, 60°, and 90°. ($x=0.5$, mixed magnetic and quadrupole.)

$$\frac{x}{1-x}=\frac{A}{P}\frac{2I}{I^2-((\frac{1}{4}))} \tag{19}$$

(Bowden *et al.*[5]). Also included in the diagram are lines of constant W, where W is essentially the strength of the nuclear Hamiltonian divided by kT. [For the special case of $x=1.0$, $W=(A/2I)/kT$.] Note that the temperature isotherms ($W \propto 1/T$) are simply parallel straight lines of slope $1/6^{1/2}$. The slope is independent of both the canting angle β and the particular values of the statistical tensors ρ_0^2 and ρ_2^2. This, at first, rather surprising result is easily verified on forming the derivative

$$\partial\bar{\rho}_2^{2'}/\partial\bar{\rho}_0^{2'}=(\partial\bar{\rho}_2^{2}/\partial\beta)/(\partial\bar{\rho}_0^{2'}/\partial\beta)$$

$$=\frac{1}{6^{1/2}}\frac{[\rho_2^2+(\frac{3}{2})^{1/2}\rho_0^2]}{[\rho_2^2+(\frac{3}{2})^{1/2}\rho_0^2]}\frac{\sin\beta\cos\beta}{\sin\beta\cos\beta}=\frac{1}{6^{1/2}}\ . \tag{20}$$

Such diagrams could be used, for example, to determine the angle β between the nuclear spins, if the temperature T and the nuclear hyperfine parameters A and P are known.

Turning now to statistical tensors of rank 4, we find using the transformation matrices defined $\alpha=\gamma=\frac{1}{2}\pi$ and β, that

$$\bar{\rho}_4^{4'}=(\rho_4^4)_{n=1,2}=\frac{1}{8}(1+6\cos^2\beta+\cos^4\beta)\rho_4^4$$
$$-\frac{7^{1/2}}{4}\sin^2\beta(1+\cos^2\beta)\rho_2^4$$
$$+\frac{1}{8}\left(\frac{35}{2}\right)^{1/2}\sin^4\beta\rho_0^4\ , \tag{21}$$

$$\bar{\rho}_2^{4'}=(\rho_2^4)_{n=1,2}=-\frac{7^{1/2}}{4}\sin^2\beta(1+\cos^2\beta)\rho_4^4$$
$$+\frac{1}{2}(7\cos^4\beta-6\cos^2\beta+1)\rho_2^4$$
$$-\frac{1}{4}\left(\frac{5}{2}\right)^{1/2}(1-\cos^2\beta)(7\cos^2\beta-1)\rho_0^4 \tag{22}$$

and

$$\bar{\rho}_0^{4'}=(\rho_0^4)_{n=1,2}=\frac{1}{4}\left(\frac{35}{2}\right)^{1/2}\sin^4\beta\rho_4^4$$
$$-\frac{1}{2}\frac{5}{2}(1-\cos^2\beta)(7\cos^2\beta-1)\rho_2^4$$
$$+\frac{1}{8}(35\cos^4\beta-30\cos^2\beta+3)\rho_0^4\ . \tag{23}$$

Diagrams for these statistical tensors as a function of β are best presented in the form of two 2-dimensional plots $\bar{\rho}_2^{4'}$ vs $\bar{\rho}_0^{4'}$ and $\bar{\rho}_4^{4'}$ vs $\bar{\rho}_0^{4'}$, as shown in Figs. 3(a) and 3(b), respectively. Once again use has been made of the tabulated statistical-tensor tables of Bowden *et al.*[5], for the special case of $I=3$ and $x=0.5$. Note that the temperature isotherms, in both diagrams, are strongly curved, in marked contrast to those of $\bar{\rho}_2^2$ vs $\bar{\rho}_0^2$. In Sec. IV, however, we show that the isotherms for statistical tensors of rank 4 are parallel straight lines, if the nuclear-spin structure possesses a fourfold symmetric axis.

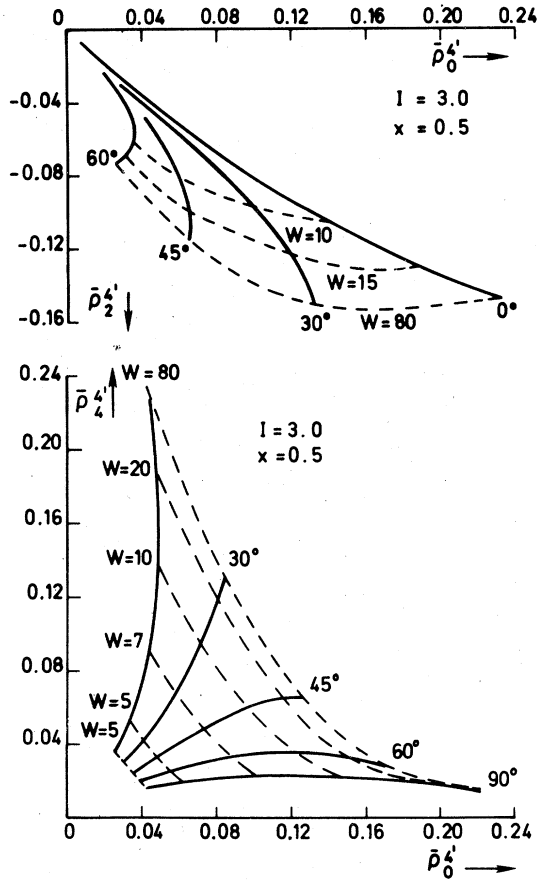

FIG. 3. Statistical-tensor diagrams of $\bar{\rho}_2^{4'}$ vs $\bar{\rho}_0^{4'}$ and $\bar{\rho}_4^{4'}$ vs $\bar{\rho}_0^{4'}$ for a twofold symmetric nuclear-spin structure with $\beta=0°$, 30°, 45°, 60°, and 90°. ($x=0.5$, mixed magnetic and quadrupole.)

IV. FOURFOLD SYMMETRIC SPIN CONFIGURATION

An example of a four-fold symmetric nuclear-spin configuration may be seen in Fig. 4. Note that for equal numbers of nuclei, the γ-ray emission pattern from the nuclear-spin arrangements of Figs. 4(a) and (b) are identical.

The appropriate average statistical tensor for four-fold symmetry is given by

$$\bar{\rho}_q^{\lambda}=\tfrac{1}{4}[\rho_q^{\lambda}(\beta)+\rho_q^{\lambda}(-\beta)+\rho_q^{\lambda}(\pi+\beta)+\rho_q^{\lambda}(-\pi-\beta)] . \tag{24}$$

Thus for $\lambda=2$ we have

$$\bar{\rho}_2^{2'}=\tfrac{3}{4}\rho_2^2-\tfrac{1}{4}(\tfrac{3}{2})^{1/2}\rho_0^2 \tag{25}$$

and

$$\bar{\rho}_0^{2'}=-\tfrac{1}{2}(\tfrac{3}{2})^{1/2}\rho_2^2+\tfrac{1}{4}\rho_0^2 , \tag{26}$$

which leads to the result

$$\bar{\rho}_2^{2'}/\bar{\rho}_0^{2'}=-(\tfrac{3}{2})^{1/2} . \tag{27}$$

A plot of $\bar{\rho}_2^{2'}$ vs $\bar{\rho}_0^{2'}$ is therefore a straight line of slope $-(\frac{3}{2})^{1/2}$. This result is formally equivalent to that of a pure quadrupole interaction directed along the x′ axis of Fig. 4(a) or (b). However, it should be possible, in practice, to distinguish between these two rather different physical situations, by virtue of their temperature dependence. For example, in the high-temperature limit $\bar{\rho}_0^2 \propto 1/T\ (1/T^2)$ for a pure quadrupole (magnetic) interaction.

For $\lambda=4$ we have

$$\bar{\rho}_4^{4'}=\frac{1}{16}(8+\sin^4\beta+\cos^4\beta)\rho_4^4 - \frac{7^{1/2}}{8}(1+2\sin^2\beta\cos^2\beta)\rho_2^4 + \frac{1}{16}\left(\frac{35}{2}\right)^{1/2}(\sin^4\beta+\cos^4\beta)\rho_0^4 , \tag{28}$$

$$\bar{\rho}_2^{4'}=-\frac{7^{1/2}}{8}(1+2\sin^2\beta\cos^2\beta)\rho_4^4 + \frac{1}{4}[7(\sin^4\beta+\cos^4\beta)-4]\rho_2^4 - \frac{1}{8}\left(\frac{5}{2}\right)^{1/2}[6-7(\sin^4\beta+\cos^4\beta)]\rho_0^4 , \tag{29}$$

and

$$\bar{\rho}_0^{4'}=\frac{1}{8}\left(\frac{35}{2}\right)^{1/2}(\sin^4\beta+\cos^4\beta)\rho_4^4 - \frac{1}{4}\left(\frac{5}{2}\right)^{1/2}[6-7(\sin^4\beta+\cos^4\beta)]\rho_2^4 + \frac{1}{16}[35(\sin^4\beta+\cos^4\beta)-24]\rho_0^4 . \tag{30}$$

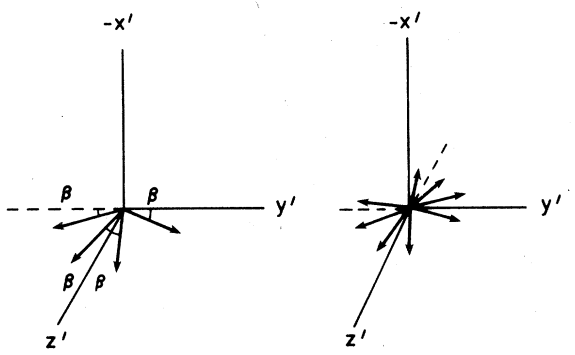

FIG. 4. Fourfold symmetric nuclear-spin structure.

These equations reveal that we have

$$\partial\bar{\rho}_4^4/\partial\bar{\rho}_0^4=(\partial\bar{\rho}_4^4/\partial\beta)/(\partial\bar{\rho}_0^4/\partial\beta)=1/70^{1/2} \quad (31)$$

and

$$\partial\bar{\rho}_2^4/\partial\bar{\rho}_0^4=(\partial\bar{\rho}_2^4/\partial\beta)(\partial\bar{\rho}_0^4/\partial\beta)=\left(\frac{2}{5}\right)^{1/2}. \quad (32)$$

Consequently, for nuclear-spin arrangements possessing fourfold rotational symmetry, temperature isotherms in $\bar{\rho}_4^4$ vs $\bar{\rho}_0^4$ and $\bar{\rho}_2^4$ vs $\bar{\rho}_0^4$ diagrams, are simply parallel straight lines, as illustrated in Figs. 5 and 6 for $x=1.0$ and 0.5, respectively. Also included in Figs. 6(a) and (b), for comparison purposes, are the straight lines $\rho_2^4/\rho_0^4=-10^{1/2}/3$ and $\rho_4^4/\rho_0^4=\frac{1}{3}(35/2)^{1/2}$, which corresponds to the pure quadrupole interaction $x=0.0$.

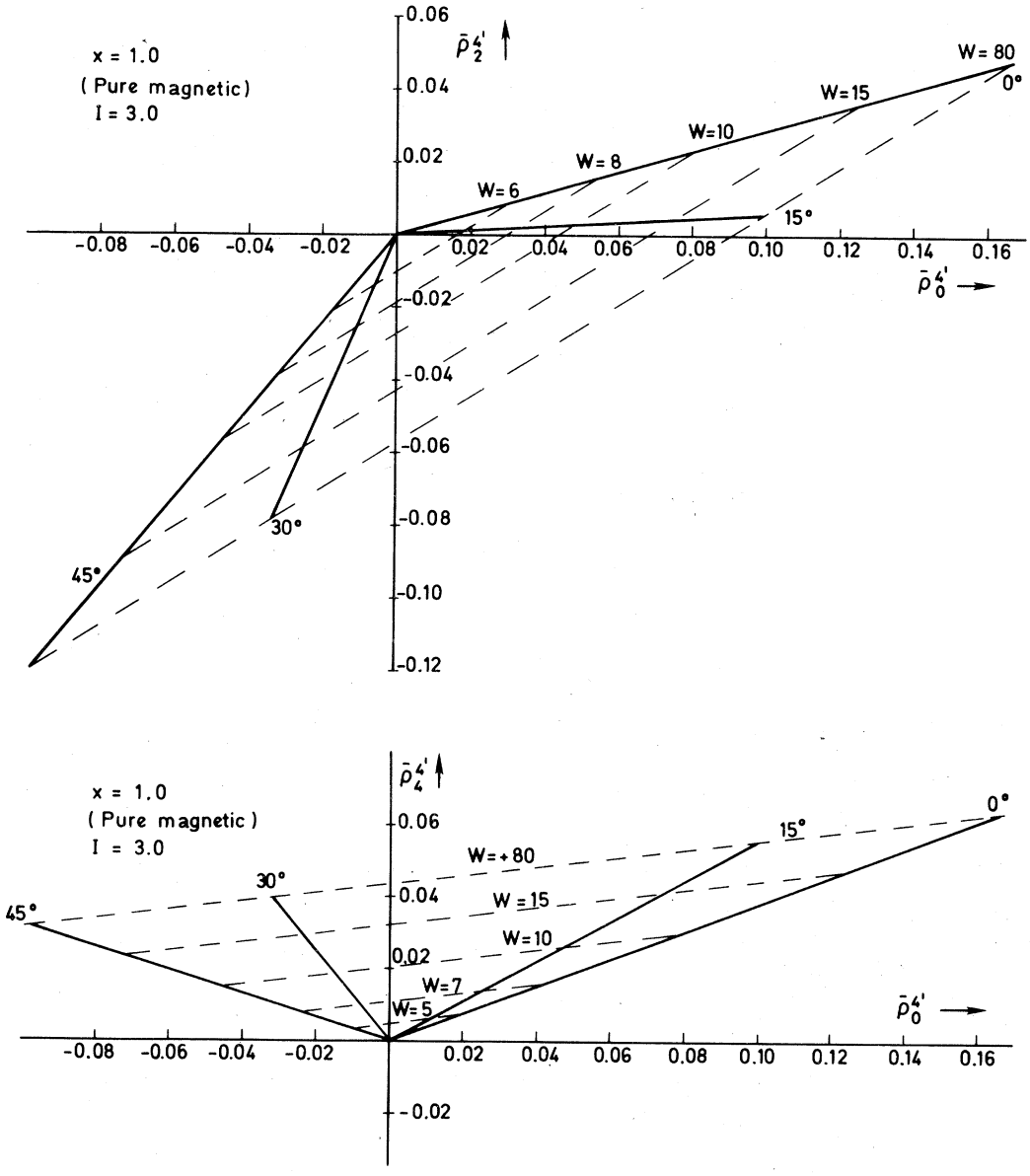

FIG. 5. Statistical tensor diagrams of $\bar{\rho}_2^{4'}$ vs $\bar{\rho}_0^{4'}$ and $\bar{\rho}_4^{4'}$ vs $\bar{\rho}_0^{4'}$ for a fourfold symmetric nuclear-spin structure with $\beta=0°$, 15°, 30°, and 45°. ($x=1.0$, pure magnetic.)

V. THREEFOLD, HEXAGONAL, AND SPIRAL NUCELAR-SPIN CONFIGURATIONS

The average statistical tensor for the threefold symmetric nuclear-spin configuration is given by

$$\bar{\rho}_q^{\lambda'} = \frac{1}{3}[\rho_q^\lambda(\beta=0) + \rho_q^\lambda(\beta=60°) + \rho_q^\lambda(\beta=-60°)] \ . \tag{33}$$

For $\lambda=2$ we have

$$\bar{\rho}_2^{2'} = \frac{3}{4}\rho_2^2 - \frac{1}{4}(\tfrac{3}{2})^{1/2}\rho_0^2 \ , \tag{34}$$

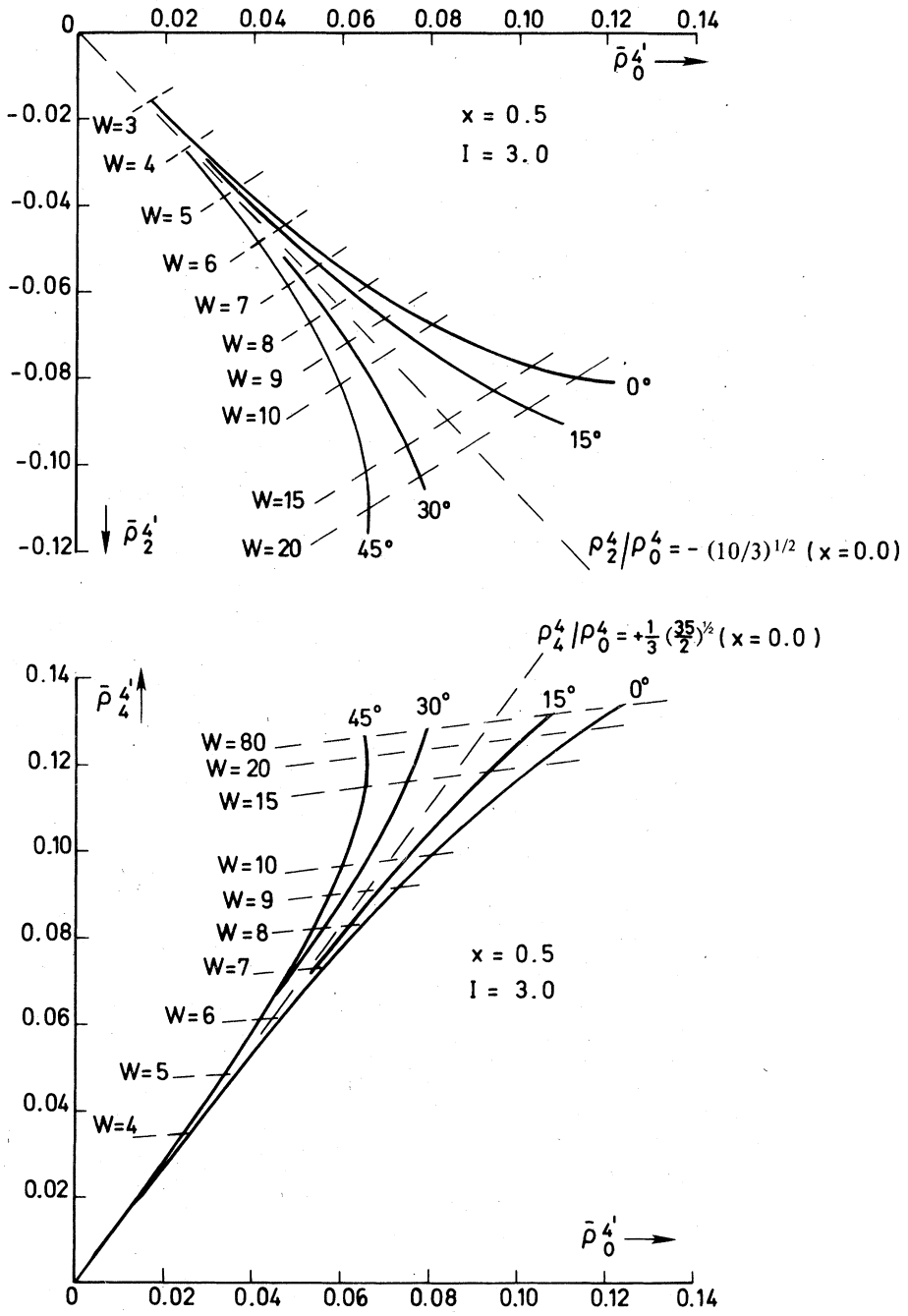

FIG. 6. Statistical tensor diagram of $\bar{\rho}_2^{4'}$ vs $\bar{\rho}_0^{4'}$ and $\bar{\rho}_4^{4'}$ vs $\bar{\rho}_0^{4'}$ for a fourfold symmetric nuclear-spin structure with $\beta=0°$, 15°, 30°, and 45°. ($x=0.5$, mixed magnetic and quadrupole.)

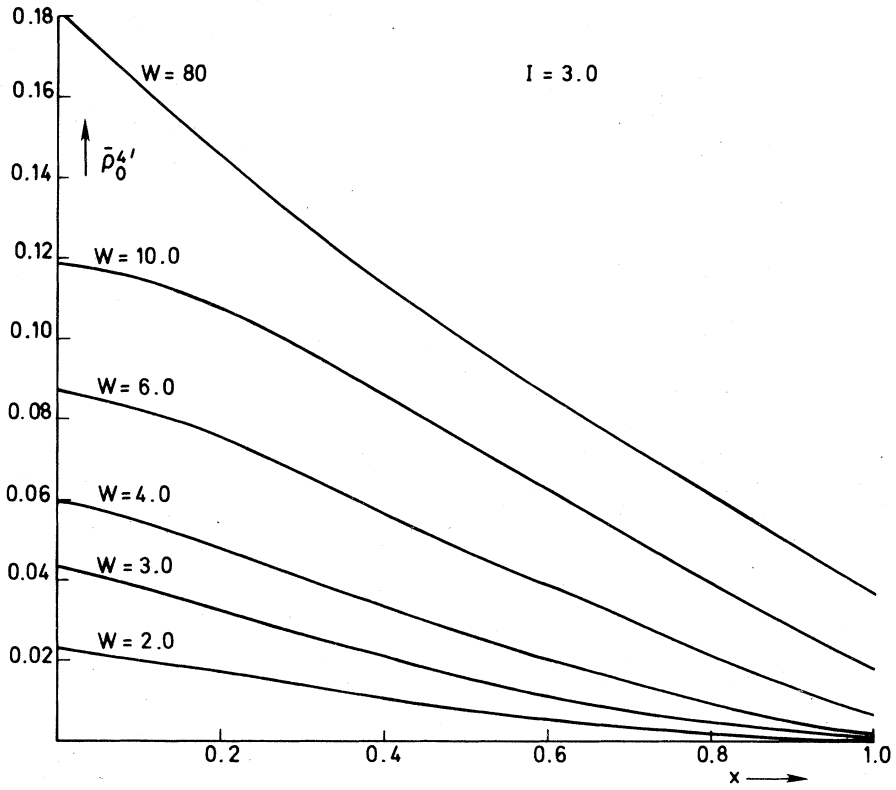

FIG. 7. Statistical tensor plot of $\bar{\rho}_0^{4'}$ vs x for a threefold symmetric nuclear-spin structure.

$$\bar{\rho}_0^{2'} = -\tfrac{1}{2}\left(\tfrac{3}{2}\right)^{1/2}\rho_2^2 + \tfrac{1}{4}\rho_0^2 \tag{35}$$

and

$$\bar{\rho}_1^{2'} \equiv 0 \ . \tag{36}$$

Thus, once again we have

$$\bar{\rho}_2^{2'}/\bar{\rho}_0^{2'} = -\left(\tfrac{3}{2}\right)^{1/2} \ , \tag{37}$$

which is formally equivalent to either (i) a pure axially symmetric quadrupole interaction directed along the x′ axis, or (ii) the fourfold nuclear-spin arrangement of Sec. IV.

For $\lambda = 4$ we find

$$\bar{\rho}_4^{4'} = \frac{35}{8^2}\rho_4^4 - \frac{5(7)^{1/2}}{4.8}\rho_2^4 + \frac{3}{8^2}\left(\frac{35}{2}\right)^{1/2}\rho_0^4 \ , \tag{38}$$

$$\bar{\rho}_2^4 = \frac{-5(7)^{1/2}}{4.8}\rho_4^4 + \frac{5}{2.8}\rho_2^4 - \frac{3}{4.8}\rho_0^4 \tag{39}$$

and

$$\bar{\rho}_0^4 = \frac{3}{4.8}\left(\frac{35}{2}\right)^{1/2}\rho_4^4 - \frac{3}{2.8}\left(\frac{5}{2}\right)^{1/2}\rho_2^4 + \frac{9}{8^2}\rho_0^4 \ , \tag{40}$$

which give rise to the ratios

$$\bar{\rho}_4^{4'}/\bar{\rho}_0^{4'} = \tfrac{1}{3}(35/2)^{1/2} \tag{41}$$

and

$$\bar{\rho}_2^{4'}/\bar{\rho}_0^{4'} = -10^{1/2}/3 \ . \tag{42}$$

Thus, it is only necessary to determine $\bar{\rho}_0^{4'}$ in order to characterize the fourth-order multipole-emission pattern. As an illustration, we show in Fig. (7) $\bar{\rho}_0^{4'}$ vs x for various values of W ($\propto 1/T$). Note also that the ratios, given by Eqs. (41) and (42), are also obtained for a pure quadrupole interaction directed along the x′ axis.[5]

Finally we remark without proof that Eqs. (34)–(42) also hold for spiral-spin configurations, in which the angle β, between adjacent ferromagnetic sheets is incommensurate with the lattice. This situation is realized, for example, in the rare-earth metal holmium.[6] We may conclude therefore that nuclear-orientation experiments involving $M1$ and $E2$ transitions are inherently incapable of distinguishing between incommensurate spirals and spin configurations which possess a threefold symmetry axis. This comment however, does not necessarily apply to distorted spiral-spin arrangements, which may, for example, possess an overall twofold symmetry axis.

VI. DISCUSSION

In the past, nuclear-orientation experiments have traditionally been used to extract information concerning nuclear hyperfine fields at solute atoms, using either brute force methods or strong magnetic hyperfine fields in ferromagnet hosts. However nuclear-orientation methods can also be used to study phenomena such as (i) spin-flop transitions in antiferromagnetic compounds,[7] (ii) spin reorientations, (iii) field-induced spiral-fan-ferromagnetic transitions, etc. Moreover with the increasing availability of single-crystal rare-earth metal and intermetallic compounds, a wide variety of spin structures is now available for study. In general, of course, magnetic spin configurations are best examined using neutron scattering techniques. However, it is anticipated that nuclear-orientation experiments will play an important role in the investigation of (i) compounds which possess very low ordering temperatures; (ii) spin directions at dilute impurity atoms in magnetically ordered hosts; and (iii) compounds which possess atoms with high neutron-absorption cross sections.

ACKNOWLEDGMENTS

The support of the Science Research Council is gratefully acknowledged, and G. J. Bowden would like to thank members of the Clarendon Laboratory for their kind hospitality during the course of this work.

---

*Permanent Address: School of Physics, Univ. of New South Wales, Kensington, NSW 2033, Australia.

[1]R. M. Steffen and K. Alder, *The Electromagnetic Interaction in Nuclear Spectroscopy* (North-Holland, Amsterdam, 1975), p. 505.
[2]U. Fano, Phys. Rev. 90, 577 (1953).
[3]U. Fano, Rev. Mod. Phys. 29, 76 (1957).
[4]A. R. Edmonds, *Angular Momentum in Quantum Mechanics*, 2nd ed. (Princeton University, Princeton, New Jersey, 1960).
[5]G. J. Bowden, I. A. Campbell, N. Nambudripad, and N. J. Stone, Phys. Rev. B 20, 352 (1979) (preceding paper).
[6]W. C. Koehler, in *Magnetic Properties of Rare Earth Metals*, edited by R. J. Elliott (Plenum, New York, 1972), p. 81.
[7]B. G. Turrell, P. D. Johnston, and N. J. Stone, J. Phys. C 5, L197 (1972).